illustrated in Figure 7, we feel, bodes poorly for the development of a simple universal scale of free radical substituent effects.

M. On the Origin of the Large *o*-Amino and *o*-Hydroxyl Effects. The most probable explanation for the large ortho effect of both hydroxyl and amino is the presence of a strong bond between the H atom on the substituent and the phenoxyl oxygen in the radical.

The present experiments measure, in effect, the change in Gibbs energy caused by the substituent. Since any H-bonding in the radical would reduce the reaction entropy (and therefore A factor for dissociation), the actual bonding enthalpy should be even larger than the reported ΔBDE. Assuming that this bonding increases the barrier of rotation from 0 to ca. 8 kcal mol^{-1}, and then using Pitzer's tables,[42] we estimate that an additional 3 kcal mol^{-1} should be added to the reaction enthalpy from this effect. Thus, the H-bonding energy in the *o*-hydroxyphenoxy and *o*-aminophenoxy radicals is estimated to be ca. 10 kcal mol^{-1} greater than in the parent molecules. These are very strong hydrogen bonds.

VI. Summary

We have determined the effects of a number of substituents on the O–CH_3 bond in anisoles. The range of ΔBDE (kcal mol^{-1}) from this and previous studies for ortho substituents was −0.2 to −7.4, for para 1.2 to −3.9, and for meta 1.2 to −1.1. In the ortho and para positions, electron-donating substituents ($\sigma^+ < 0$) significantly weakened bonds; electron-accepting groups ($\sigma^+ > 0$) had significantly less effect but strengthened bonds somewhat when in the para position. Meta substituents showed no clear systematic trends.

An exceptionally large bond weakening was observed for the *o*-NH_2 substituent, quite similar to the value for the *o*-OH group reported recently. It is tentatively proposed that this effect is due to an unexpectedly strong H bond in the radical. We calculate that such a bond is ca. 10 kcal mol^{-1} stronger than in the molecule.

Phenolic H-abstraction rates for para substituents show some correlation with ΔBDE, but are correlated much better by σ^+ substituent constants. This is interpreted as consequence of significant polar kinetic effects in the H-abstraction reactions.

ΔBDE values for both ortho and para substituents are well correlated by ESR hyperfine coupling constants of substituted phenoxy radicals. However, unlike seemingly related effects observed for substituted benzyl radicals, stabilizing substituents decrease the apparent alternation of hfcc's (spin density) in the radical rather than simply withdrawing density from the other sites.

ΔBDE correlates poorly with existing measures of substituent effects for carbon-centered radicals. This is somewhat surprising since in terms of odd-electron density, phenoxy radicals are essentially carbon centered radicals.

Acknowledgment. This work was supported by a grant from the Gas Research Institute.

Registry No. *o*-NH_2PhOCH_3, 90-04-0; *o*-$HOPhOCH_3$, 90-05-1; *o*-$CH_3OPhOCH_3$, 91-16-7; *o*-CH_3PhOCH_3, 578-58-5; *o*-$HOCH_2PhOCH_3$, 612-16-8; $PhOCH_3$, 100-66-3; *o*-$FPhOCH_3$, 321-28-8; $(F)_5PhOCH_3$, 389-40-2; *o*-$ClPhOCH_3$, 766-51-8; *o*-$BrPhOCH_3$, 578-57-4; *o*-$CH_3COPhOCH_3$, 579-74-8; *o*-$H_2C{=}CHPhOCH_3$, 612-15-7; *o*-$CNPhOCH_3$, 6609-56-9; *o*-$O_2NPhOCH_3$, 91-23-6; *m*-NH_2PhOCH_3, 536-90-3; *m*-$HOPhOCH_3$, 150-19-6; *m*-$CH_3OPhOCH_3$, 151-10-0; *m*-CH_3PhOCH_3, 100-84-5; *m*-$FPhOCH_3$, 456-49-5; *m*-$ClPhOCH_3$, 2845-89-8; *m*-$CH_3COPhOCH_3$, 586-37-8; *m*-$CNPhOCH_3$, 1527-89-5; *m*-$O_2NPhOCH_3$, 555-03-3; *p*-NH_2PhOCH_3, 104-94-9; *p*-$HOPhOCH_3$, 150-76-5; *p*-$CH_3OPhOCH_3$, 150-78-7; *p*-CH_3PhOCH_3, 104-93-8; *p*-$FPhOCH_3$, 459-60-9; *p*-$ClPhOCH_3$, 623-12-1; *p*-$CH_3COPhOCH_3$, 100-06-1; *p*-$CNPhOCH_3$, 874-90-8; *p*-$O_2NPhOCH_3$, 100-17-4; 1-methyoxynaphthalene, 2216-69-5; 2-methoxynaphthalene, 93-04-9.

(42) Lewis, G. N.; Randall, M.; Pitzer, K. S.; Brewer, L. *Thermodynamics*, 2nd ed.; McGraw-Hill: New York, 1961; p 446.

Real-Time Reaction Monitoring by Continuous-Introduction Ion-Spray Tandem Mass Spectrometry

Edgar D. Lee,[†] Wolfgang Mück,[†,‡] Jack D. Henion,*[,†] and Thomas R. Covey[§]

Contribution from Drug Testing and Toxicology, New York State College of Veterinary Medicine, Cornell University, 925 Warren Drive, Ithaca, New York 14850, and SCIEX, 55 Glencameron Road, Thornhill, Ontario, Canada L3T 1P2. *Received November 18, 1988*

Abstract: A temperature-controlled reaction vessel was closely coupled to the ion-spray LC/MS interface on an atmospheric pressure ionization, triple quadrupole mass spectrometer and used to study mechanistic and kinetic aspects of reactions taking place in solution. Free access to the reaction vessel and temperature control as well as minimal sample consumption make continuous-introduction ion-spray mass spectrometry a useful approach for real-time measurement of reactions. The reaction medium, reactants, and products were transferred to the ion source of the mass spectrometer from the reaction vessel in less than 1 s. A variety of model reactions have been investigated to demonstrate the feasibility and potential for continuous-introduction ion-spray mass spectrometry for real-time reaction monitoring. The half-life for the solvolysis of methandrostenolone sulfate in aqueous medium and the Michaelis–Menten constant of the enzymatic hydrolysis of *O*-nitrophenyl β-D-galactopyranoside by lactase were determined. The enzymatic hydrolysis of dynorphin 1–8 by α-chymotrypsin and leucine aminopeptidase and the reduction of the disulfide bridge in oxytocin with β-mercaptoethanol were obtained on-line to emphasize the technique's capability for peptide sequencing and structural elucidation.

The study of reaction mechanisms and kinetics is fundamentally important for characterizing synthetic pathways of chemical reactions and for understanding biochemical processes occurring in life science. Nearly all known analytical techniques have been used to follow reaction mechanisms and kinetics.[1] The objectives and challenges imposed by the complexity and speed of the reaction under investigation require instrumentation possessing the necessary selectivity and sensitivity to follow the reaction to completion.

* Author to whom correspondence should be addressed.
† Cornell University.
‡ On leave from the Department of Pharmacy and Food Chemistry, Würzburg University, 8700 Würzburg, FRG.
§ SCIEX.

(1) Zuman, P.; Patel. R. C. *Techniques in Organic Reaction Kinetics*; Wiley: New York, 1984.

0002-7863/89/1511-4600$01.50/0

The high degree of specificity of mass spectrometry for the identification of molecular species in mixtures and its excellent sensitivity are attractive for studying reaction mechanism and kinetics. Mass spectrometry and, in particular, Fourier transform mass spectrometry have been the most powerful techniques for monitoring reaction mechanisms of gas-phase chemistry.[2] The assumption that prior vaporization is a prerequisite of ionization prevented mass spectrometry from playing an important role for the real-time investigation of liquid-phase reactions. It has not been until the advent of mild ionization techniques such as fast atom bombardment (FAB),[3] thermospray,[4] and electrospray[5] that the mass spectrometer has been able to monitor reactions occurring in solution.

Dynamic FAB mass spectral analysis has been reported for both enzymatic and nonenzymatic reactions.[6] Trypsin-catalyzed hydrolysis[7,8] and glutathione transferase catalyzed conjugation reactions[9] could be observed real time by placing the reaction mixtures directly onto the FAB probe followed by immediate insertion of the probe into the ion source of the mass spectrometry. This on-line method had the advantages of using a small amount of sample, being fast, and allowing many sampling times for the mass spectral acquisition. However, the requirement in FAB for a high-percentage glycerol matrix imposes severe restrictions on the formulation of suitable matrix conditions without affecting enzyme activities or chemical reactivities. Decreases in reaction rate or total inactivation after a few minutes have been reported due to the increasing glycerol content of the sample from evaporation of water.[8] The development of flow FAB[10] improved this situation by allowing the continuous introduction of higher aqueous buffer systems. Both direct flow of reaction solution into the source, if compatible to FAB analysis, and flow injection of timed aliquots of the reaction medium into a glycerol-containing aqueous carrier have been reported by Caprioli and co-workers.[11]

Thermospray mass spectrometry has also been used for reaction monitoring by using columns containing immobilized enzymes prior to introduction into the ion source,[12,13] and by direct coupling of an electrochemical cell to the mass spectrometer via the thermospray LC interface.[14,15] However, the high liquid flow rates required for thermospray[4] lead to high volume consumption, making the use of on-line monitoring of a small reaction vessel impractical. Additionally, thermospray ionization requires heat, which may have an adverse effect on the reaction, particularly if either the substrate or product is thermally sensitive.

Electrospray, on the other hand, which has recently gained renewed interest as an efficient interface for liquid chromatography[16] and capillary electrophoresis,[17] requires very low flow rates (1–10 μL/min), and ionization by ion evaporation[18] occurs at atmospheric pressure. Since ionization is at atmospheric pressure, the reaction vessel can be coupled close to the mass spectrometer with a minimal time difference between the reaction and detection while the operator maintains free access to the vessel during operation of the mass spectrometer. Ion spray (pneumatically assisted electrospray) improves electrospray by incorporation of pneumatic nebulization to assist the nebulization process.[19] This improves the sensitivity and stability of electrospray particularly when higher liquid flow is required and high percentages of aqueous buffer are used.[19] For negative ion operation the nebulizing gas acts as an electron scavanger and suppresses any discharge behavior.[19]

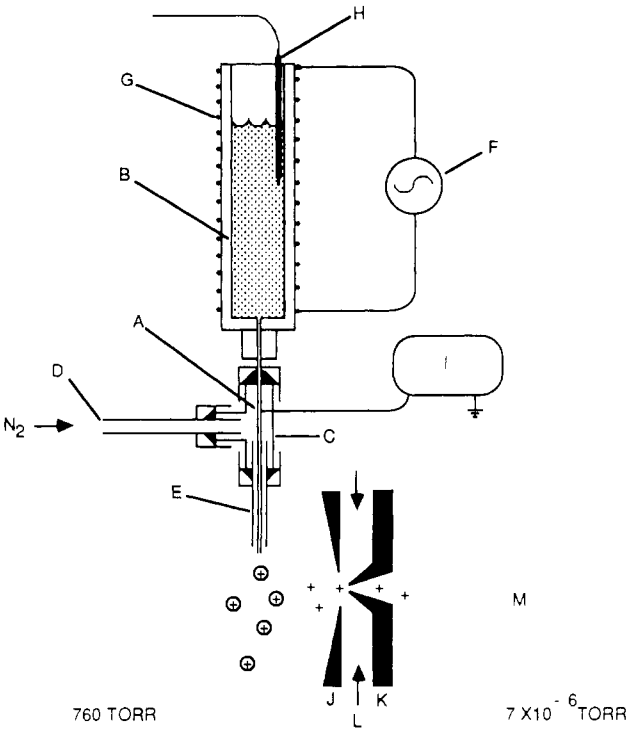

Figure 1. Schematic illustration of the continuous-introduction ion-spray interface: (A) electrospray electrode, (B) reaction chamber, (C) $^1/_{16}$-in. tee, (D) nebulizing gas inlet, (E) coaxial tube around electrode, (F) powerstat, (G) coiled nichrome wire, (H) thermocouple, (I) high-voltage power supply, (J) interface plate of mass spectrometer, (K) conical skimmer orifice of mass spectrometry, (L) nitrogen curtain gas, (M) mass analyzer.

For these reasons we have developed and report the first use of a continuous-introduction ion-spray inlet with mass spectrometry for real-time monitoring of reactions as they proceed to completion. The purpose of the study was not to show highly sophisticated reaction studies but to introduce electrospray ionization at atmospheric pressure as a tool for continuously monitoring reactions in solution by mass spectrometry. The potential of this new analytical approach was demonstrated using simple, well-understood model systems.

Experimental Section

Apparatus. A schematic illustration of the instrumentation used for this work is shown in Figure 1. The continuous-introduction ion-spray inlet was based on the ion-spray LC/MS interface reported previously.[19] The electrospray electrode (A) through which the reaction medium flowed was a custom-made 100-μm-i.d. × 200-μm-o.d. stainless steel

(2) *Gas Phase Ion Chemistry*; Bowers, M., Ed.; Academic Press: New York, 1979.
(3) Barber, M.; Bordoli, R. S.; Elliot, G. J.; Sedgwick, R. D.; Tyler, A. N. *Anal. Chem.* **1982**, *54*, 645–657A.
(4) Blakely, C. R.; Vestal, M. L. *Anal. Chem.* **1983**, *55*, 750–754.
(5) Yamashita, M.; Fenn, J. B. *J. Phys. Chem.* **1984**, *88*, 4451–4459.
(6) Caprioli, R. M. Fast-atom-bombardment Mass Spectrometry. Rose, M. E., Ed.; *Mass Spectrometry*; The Royal Society of Chemistry: London, 1985.
(7) Caprioli, R. M.; Smith, L. A. *Biomed. Mass Spectrom.* **1983**, *10*, 98–102.
(8) Smith, L. A.; Caprioli, R. M. *Biomed. Mass Spectrom.* **1984**, *11*, 392–395.
(9) Heidmann, M.; Fonrobert, P.; Przybylski, M.; Platt, K. L.; Seidel, A.; Oesch, F. *Biomed. Mass Spectrom.* **1987**, *15*, 329–332.
(10) Caprioli, R. M.; Fan, T.; Cottrell, J. S. *Anal. Chem.* **1986**, *58*, 2949–2954.
(11) Moore, W. T.; Fan, T.; Caprioli, R. M. Determination of Enzymatic Reaction Parameters by On-Line FABMS. Presented at the 35th ASMS Conference on Mass Spectrometry and Allied Topics, Denver, CO, May 24–29, 1987.
(12) Kim, H. Y.; Pilosof, D.; Dyckes, D. F.; Vestal, M. L. *J. Am. Chem. Soc.* **1984**, *106*, 7304–7309.
(13) Stachowiak, K.; Wilder, C.; Vestal, M. L.; Dyckes, D. F. *J. Am. Chem. Soc.* **1988**, *110*, 1758–1765.
(14) Hambitzer, G.; Heitbaum, J. *Anal. Chem.* **1986**, *58*, 1067–1070.
(15) Getek, T. A.; Kormacher, W. A. The Study of Acetaminophen Conjugate Formation by Oxidative Electrochemistry and Thermospray Mass Spectrometry. Proceedings of the 36th ASMS Conference on Mass Spectrometry and Allied Topics, San Francisco, CA, June 5–10, 1988.
(16) Whitehouse, C. M.; Dreyer, R. N.; Yamashita, M.; Fenn, J. B. *Anal. Chem.* **1985**, *57*, 675–679.
(17) Smith. R. D.; Barinaga, C. J.; Udseth, H. R. *Anal. Chem.* **1988**, *60*, 1948–1952.
(18) Thomson, B. A.; Iribarne, J. V. *J. Chem. Phys.* **1979**, *71*, 4451–4463.
(19) Bruins, A. P.; Covey, T. R.; Henion, J. D. *Anal. Chem.* **1987**, *59*, 2642–2646.

capillary needle with a luer end (Popper & Sons, New Hyde Park, NY) that was connected directly to a 1-mL-volume luer tip syringe barrel (B) (SGE, Austin, TX), which was used as the reaction vessel. The electrode (A) passed through a $^1/_{16}$-in. stainless steel tee (C) (SGE, Austin, TX). Nitrogen gas for assisting the electrospray nebulization was introduced through the side port (D) of the SGE tee and exited at the end of the electrospray electrode (A) at a velocity of approximately 300 m/s through a concentric 325-μm-i.d. stainless steel tube (E). The end of the electrode (A) protruded 500 μm past the end of the concentric tube (E). Temperature regulation of the reaction vessel was accomplished by applying current with a powerstat (F) (The Superior Electronic Co., Bristol, CT) across a 500-cm length of 26-gauge nichrome wire (G) coiled around the reaction vessel (B). The temperature inside the reaction vessel (B) was measured with a thermocouple (H) placed inside. A 0–10-kV voltage and current-regulated power supply (I) (Spellman, Model RHR10PN30.FG, Plainview, NY) was used to float the ion-spray interface at +3 and −3 kV for positive and negative ion operation, respectively. The interface plate (J) of the atmospheric pressure ionization source of the mass spectrometer served as the counter electrode to the ion-spray interface.

Mass Spectrometry. A SCIEX TAGA 6000E triple-quadrupole mass spectrometer (Thornhill, Ontario, Canada) equipped with an atmospheric pressure ion source was used to sample ions produced from the ion-spray interface. Ions were sampled into the vacuum for mass analysis through a 100-μm-i.d. orifice in the end of a skimmer cone (K) extended toward atmosphere. The atmospheric side of the cone (K) was bathed with a curtain of high-purity, dry nitrogen gas (L). The nitrogen curtain acted as a barrier to restrict contaminants and solvent vapor from entering the mass spectrometer vacuum. High vacuum in the analyzer region (M) of the mass spectrometer was achieved by cryogenically cooled surfaces maintained at 15–20 K surrounding the quadrupole mass filter. During routine operation the indicated high vacuum was 7×10^{-6} Torr, and during collision-induced dissociation (CID) the vacuum was 1.5×10^{-5} Torr with a target gas thickness of 230×10^{12} atoms/cm^2 of ultra-pure argon (Matheson, Secaucus, NJ) in the collision cell. A collision energy of 70 V was used for all CID experiments.

Chemicals and Reagents. Methandrostenolone sodium sulfate was purchased from Steraloids (Wilton, NH). *O*-Nitrophenyl β-D-galactopyranoside (ONPG), dynorphin 1–8, α-chymotrypsin, and leucine aminopeptidase were purchased from Sigma Chemical Co. (St. Louis, MO). The enzyme lactase was purchased from a local health food store under the trade name of Lact-Aid.[20] Oxytocin was purchased as a veterinary injectable formulation from The Butler Company (Columbus, OH). The HPLC grade water, methanol, and ammonium acetate were obtained from Fischer Scientific (Rochester, NY).

Results and Discussion

Solvolysis of Methandrostenolone Sulfate to *epi*-Methandrostenolone. A recent metabolism study of the anabolic steroid methandrostenolone in the horse indicated that two of the major metabolites found in equine urine were the sulfoconjugated parent drug and 17-*epi*-methandrostenolone.[21] It was shown that *epi*-methandrostenolone was readily formed by nucleophilic attack by water on the labile sulfate conjugate, which contradicted the concept of enzymatic epimerization suggested by others. The half-life for methandrostenolone sulfate in equine urine was determined to be 2 min at 70 °C and 16 min at 37 °C by extraction after a defined incubation time and coupled-column chromatography with UV detection.[21]

By monitoring the deprotonated molecular ion of methandrostenolone sulfate at m/z 379 with the continuous-introduction ion-spray system, we were able to observe the hydrolysis of the labile sulfate as it occurred (Figure 2). This experiment was accomplished by dissolving 1 mg of methandrostenolone sulfate in 1 mL of a water/methanol mixture (65:35, v/v) followed by transfer of the solution directly to the reaction vessel. The addition of methanol was necessary to prevent precipitation of free methandrostenolone due to its limited solubility in water. The reaction vessel was maintained at a temperature of 43 °C during the measurement. After the sample was transferred to the reaction vessel, mass spectrometric monitoring of the disappearance curve was acquired for methandrostenolone sulfate. A half-life of 4.5 min for the hydrolysis of methandrostenolone sulfate was determined from its disappearance curve, which is in good agreement with the results of the previous experiments.[21]

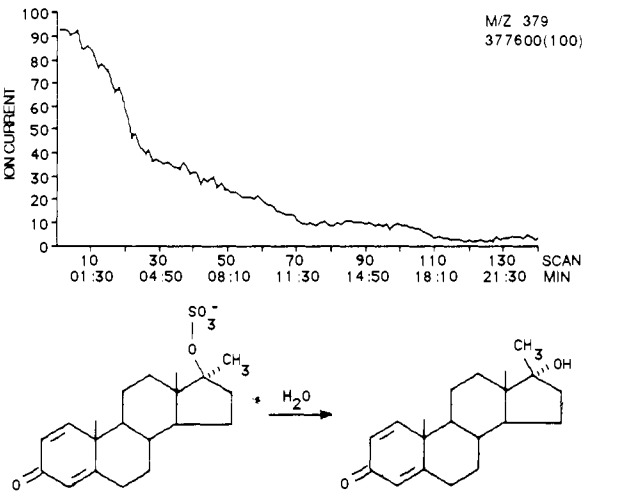

Figure 2. SIM disappearance curve for the solvolysis of methandrostenolone sulfate to *epi*-methandrostenolone. The $(M - H)^-$ ion at m/z 379 of methandrostenolone sulfate was monitored.

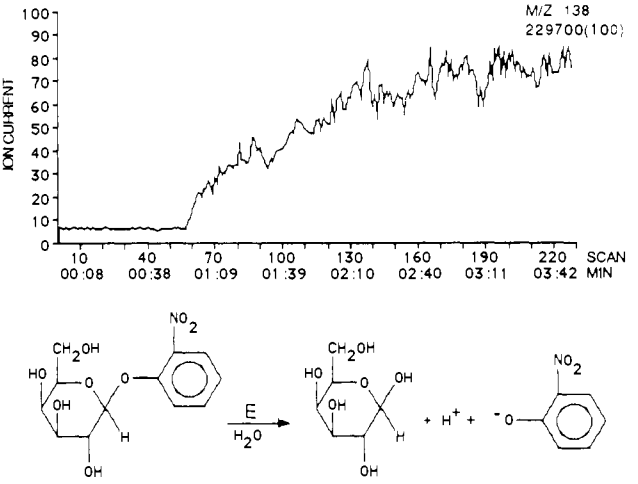

Figure 3. SIM appearance curve of *O*-nitrophenylate from the enzymatic hydrolysis of *O*-nitrophenyl β-D-galactopyranoside by lactase to galactose and *O*-nitrophenylate. The M^- ion at m/z 138 of the *O*-nitrophenylate was measured.

Enzymatic Hydrolysis of *O*-Nitrophenyl β-Galactopyranoside by Lactase. Lactase is a specific intestinal β-galactosidase that is responsible for catalyzing the hydrolysis of lactose to D-glucose and D-galactose. Russo et al.,[20] reported a simple experimental setup for the kinetic study of the enzyme lactase using the synthetic substrate, *O*-nitrophenyl β-galactopyranoside (ONPG), instead of lactose. The hydrolysis of this substrate was catalyzed by lactase and produced *O*-nitrophenylate, which was monitored with a UV/vis spectrophotometer.

This experiment was repeated with the exception that we used the continuous-introduction ion-spray inlet with an API mass spectrometer to monitor the formation of the *O*-nitrophenylate ion at m/z 138 (Figure 3). Five different concentrations (1, 2, 4, 5, and 10 mM) of OPNG were prepared in 5 mM NH_4OAc, pH 6.8; 2 drops of the commercial enzyme preparation were diluted in 20 mL of water. The appearance curve for each of the five OPNG concentrations was determined by putting a 1-mL volume of the OPNG solution in the reaction vessel (T = 30 °C) after which aquisition by the mass spectrometer was begun. After a base line was obtained, a 100-μL aliquot of the enzyme solution was added to the reaction vessel while it was stirred with an insulated pipet to prevent electrical shock from the high voltage. For each experiment the initial slope of the appearance curve was determined. The initial slope is equal to the initial rate (V) according to the Michaelis–Menten model $V = V_{max}[S]/(K_m +$

(20) Russo, S. F.; Moothart, L. *J. Chem. Educ.* **1986**, *63*, 242–243.
(21) Edlund, P. O.; Bowers, L.; Henion, J. *J. Chromatogr.* **1989**, *487*, 341–356.

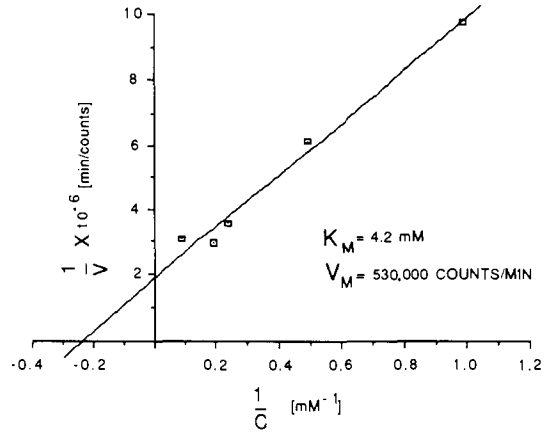

Figure 4. Lineweaver–Burke plot for the enzymatic hydrolysis of *O*-nitrophenyl β-D-galactopyranoside by lactase to galactose and *O*-nitrophenylate.

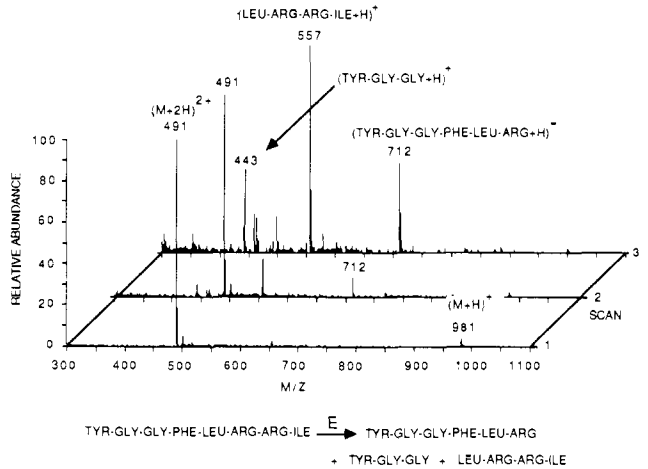

Figure 5. Ion-spray mass spectra from the enzymatic hydrolysis of dynorphin 1–8 by α-chymotrypsin taken at 0–1, 1–2, and 2–3 min during the reaction period.

[S]) where V_{max} is the maximum velocity, [S] is the initial substrate concentration, and K_m is the Michaelis–Menten constant. The results were plotted as a Lineweaver–Burke plot (Figure 4), and the V_{max} and K_m were determined to be 530 000 counts/min and 4.2 mM, respectively. The K_m is similar to 1.7 and 2.7 mM, which were reported previously and determined by other methods.[20]

Enzymatic Hydrolysis of Dynorphin 1–8 with α-Chymotrypsin and Leucine Aminopeptidase. A 10^{-4} M solution of dynorphin 1–8 and a 1 mg/mL solution of α-chymotrypsin in 5 mM acetate buffer, pH 6.8, were prepared. A total of 100 μL of the α-chymotrypsin solution was added to a 1-mL portion of the peptide solution and mixed thoroughly. This mixture was placed in the reaction vessel at room temperature, and the mass spectrometer was scanned from *m/z* 300 to 1100 at a rate of 0.8 min/scan, with one scan being acquired every 1 min. As shown (Figure 5) the protonated molecular ion at *m/z* 981 and the diprotonated molecular ion at *m/z* 491 are the prevalent ions in the first scan acquired. After 2 min these ions had given way to the ions at *m/z* 443, 557, and 712, which now dominated the mass spectrum. The ions at *m/z* 443, 557, and 712 correspond to hydrolysis of dynorphin 1–8 on both sides of the phenylalanine and between the two arginine residues. Although a considerable amount of information can be determined from a single experiment, it is usually not enough to entirely determine the sequence of an unknown peptide. This would require a series of experiments using a series of different enzymes. For example, the experiment above was repeated with the exception that the enzyme used was leucine aminopeptidase (200 μL of peptide solution to 200 μL of enzyme solution). Leucine aminopeptidase cleaved the terminal amino acid tyrosine after 7 min of reaction time (Figure 6).

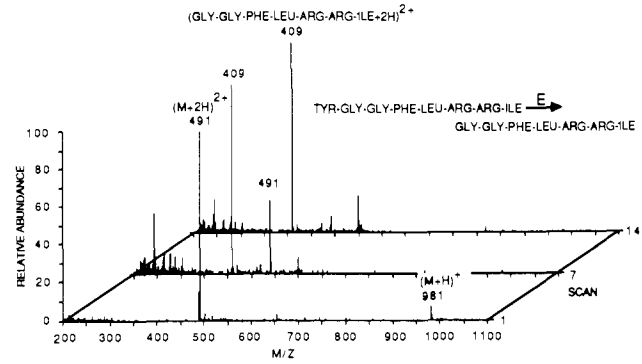

Figure 6. Ion-spray mass spectra from the enzymatic hydrolysis of dynorphin 1–8 by leucine aminopeptidase taken at 0–1, 6–7, and 13–14 min during the reaction period.

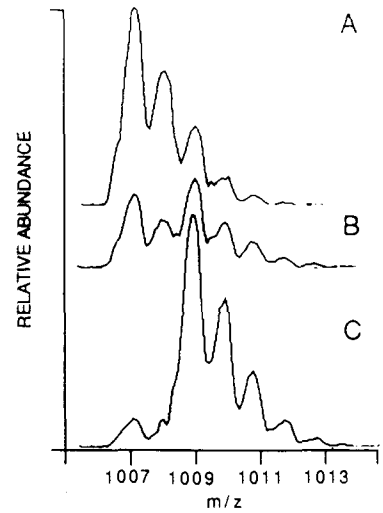

Figure 7. Ion-spray mass spectra of the molecular ion region for the reduction of oxytocin with β-mercaptoethanol: (A) oxytocin at time 0, and (B) oxytocin and reduced oxytocin at 5 min and (C) at 10 min.

Reduction of the Disulfide Bridge in Oxytocin. Disulfide bonds are important for maintaining the secondary and tertiary structure of proteins and peptides. Correct identification and placement of the disulfide bonds within an amino acid sequence are probably the most important steps in the complete structural analysis of a protein or peptide. Analysis by mass spectrometry of cystine- and cysteine-containing peptides has classically required chemical modification. With the advent of soft ionization techniques such as FAB, thermospray, and electrospray, the analysis of intact underivatized peptides is possible. Buko et al.[22] have studied several disulfide-containing peptides by FAB mass spectrometry. They were able to differentiate between the active and reduced oxytocin by observing a shift in mass of two mass units for the reduced form. The continuous-introduction ion-spray inlet allowed us to observe the reduction of the disulfide bridge in oxytocin as it occurred (Figure 7).

A 1-mL portion of a 0.04 mM oxytocin solution was mixed with 10 μL of β-mercaptoethanol and transferred to the reaction vessel of the ion-spray system, which was maintained at a temperature of 80 °C. The disappearance curve (Figure 8A) of the oxytocin and the appearance curve (Figure 8C) of reduced oxytocin gave the expected response. It is interesting to note that the appearance curve (Figure 8C) for the reduced oxytocin decreases at the start and then increases. This is a result of the A + 2 isotope[23] at *m/z* 1009 of the oxytocin being more abundant than the reduced form

(22) Buko, A. M.; Fraser, B. A. *Biomed. Mass Spectrom.* **1985**, *12*, 577–585.
(23) McLafferty, F. W. *Interpretation of Mass Spectrometry, 3rd ed.*; University Science Books: Mill Valley, CA, 1980.

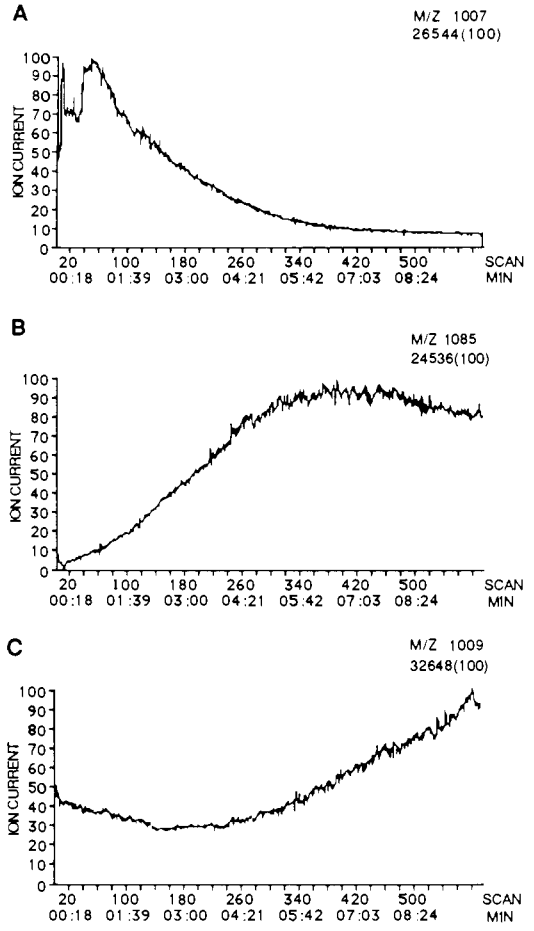

Figure 8. SIM disappearance curve for oxytocin (A), appearance curve for β-mercaptoethanol oxytocin intermediate (B), and appearance curve for reduced oxytocin (C).

of oxytocin in the early stages of the experiment (Figure 7). A reaction intermediate was also observed 77 Da higher at m/z 1085, corresponding to the addition of β-mercaptoethanol to the disulfide bridge. Similar observations have been made with FAB mass spectrometry of oxytocin,[23] though it was postulated that the intermediate was an adduct. As would be expected, the curve acquired by monitoring the intermediate product (Figure 8B) with the continuous-introduction ion-spray inlet increased with reaction time initially and then began to fall as the reduced oxytocin was formed (Figure 8C).

The MS/MS daughter-ion spectra of oxytocin, the reaction intermediate, and reduced oxytocin (Figure 9) were acquired to confirm the presence of the intermediate and to locate the position of the disulfide bridge. All three spectra contained the ion at m/z 285 as the base peak corresponding to the last three intact amino acids (Figure 9A–C). CID of oxytocin (Figure 9A) contained the daughter ion at m/z 723, which corresponded to cleavage after the second cysteine. This ion is also observed in the reduced oxytocin spectrum (Figure 9C) at a m/z of 725 and the reaction intermediate spectrum (Figure 9B) at m/z 801, which corresponds to the reduction of the disulfide bridge and the addition of the β-mercaptoethanol, respectively. Also observed in the CID mass spectrum of oxytocin are ions at m/z 323, 436, and 563. These ions are unique to the oxytocin spectrum because they all contain the intact disulfide bridge. Both the intermediate and the reduced oxytocin CID spectra contain the ions m/z 267, 508, and 622, which are consistent with the sequence of oxytocin in its reduced form and demonstrate that the β-mercaptoethanol intermediate is attached to the second cysteine within the peptide.

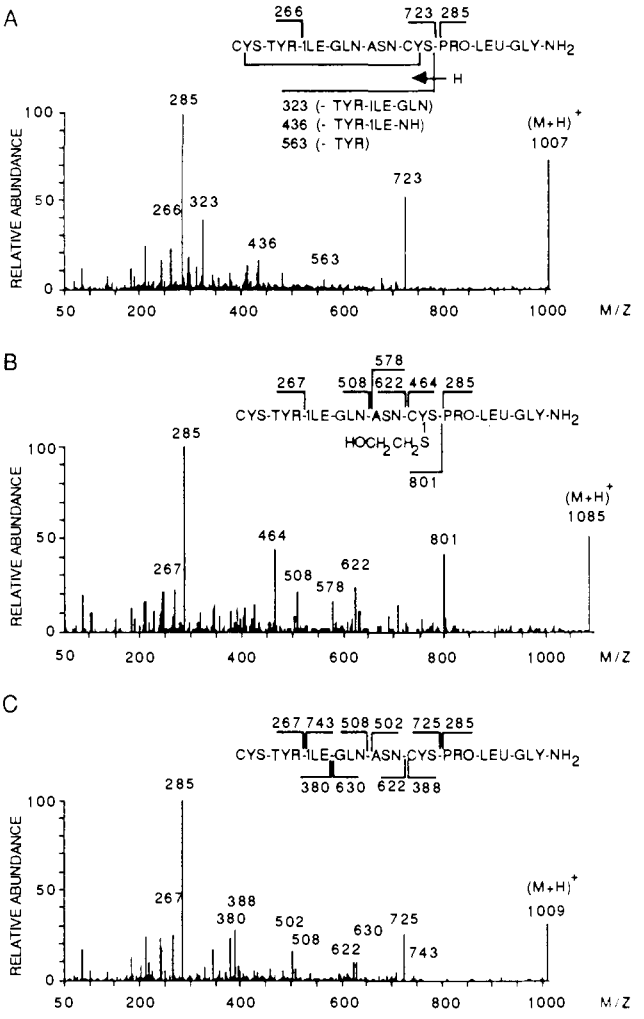

Figure 9. Daugher-ion mass spectra for the protonated molecular ions of oxytocin (A), β-mercaptoethanol oxytocin intermediate (B), and reduced oxytocin (C).

Conclusions

Real-time measurements of reactions occurring in solution by on-line mass spectrometry can be of unique value for the investigation of certain types of processes due to the inherent selectivity and sensitivity of mass spectrometry. The continuous-introduction ion-spray inlet for atmospheric pressure ionization mass spectrometry is simple in construction and use. Appearance and disapearance curves of reactive starting species, intermediates, and products are obtained in short time periods. Because the ionization occurs at atmospheric pressure, the reaction vessel can be closely coupled to the mass spectrometer, and transfer of the reaction medium from the reaction vessel is nearly instantaneous. The value of this approach is that measurement of the reaction is right after it occurs. Other attractive features that increase the utility of this approach are temperature control, free access to the reaction, and minimal sample consumption. It should be noted that there is a potential safety hazard due to the high voltage used for the electrospray process. However, one has free access to the reaction vessel if caution and a electrically insulated pipet for addition of the reagents are used. The buffer medium used can contain a wide range of different systems. This is particularly important in enzymatic reactions because many enzymes are inactivated in high organic environments. We have not explored the possibility of negative effects upon the enzymatic activity due to the high voltage, although no apparent adverse effects were observed for the reactions studied in this paper.